Aalborg Universitet

AALBORG UNIVERSITY

Conventional Synchronous Reference Frame Phase-Locked Loop Is An Adaptive Complex Filter

Golestan, S.; Guerrero, J.M.

Conventional Synchronous Reference Frame Phase-Locked Loop Is An Adaptive Complex Filter

Saeed Golestan, *Member, IEEE*, and Josep M. Guerrero, *Senior Member, IEEE*

Abstract—Despite the wide acceptance and use of the conventional synchronous reference frame phase-locked loop (SRF-PLL) no transfer function describing its actual input-output relationship has been developed so far. Arguably, the absence of such transfer function has hampered the application of SRF-PLL as a filter or controller inside the closed-loop control systems. In this paper, the transfer function describing the actual input-output relationship of the conventional SRF-PLL is presented. Using this transfer function, it is shown that the conventional SRF-PLL is a first-order adaptive complex bandpass filter. It is also shown that this transfer function can be useful for tuning of SRF-PLL parameters. The accuracy of this transfer function is confirmed through numerical results.

Index Terms—Synchronous reference frame phase-locked loop (SRF-PLL), modeling, complex filters.

I. INTRODUCTION

Owing to its simple structure, robustness, and effectiveness, the synchronous reference frame phase-locked loop (SRF-PLL) is probably the most popular and widely used technique for extraction of information about the grid fundamental component in three-phase systems [1]. Fig. 1 shows the block diagram description of this PLL. In this PLL, as shown, the stationary ($\alpha\beta$) coordinate voltages (which are obtained by applying the Clarke transformation to the three-phase voltages) are transformed to the synchronous reference frame by applying the Park transformation. The dq reference frame angular position is regulated using a feedback control loop which forces v_q to zero. Typically, a proportional-integral (PI) controller is used as the loop filter (LF). Also, to make the SRF-PLL performance insensitive to grid amplitude variations, the signal v_q is divided by an estimation of grid voltage amplitude, which can be obtained by passing v_d through a low-pass filter (LPF) [2]. The fundamental frequency positive sequence (FFPS) components are finally constructed using the extracted phase and amplitude.

To the best of the authors knowledge, no transfer function relating the input voltages to the output voltages of the conventional SRF-PLL has been developed so far. We believe the absence of such transfer function has hampered the application

S. Golestan is with the Department of Electrical Engineering, Abadan Branch, Islamic Azad University, Abadan 63178-36531, Iran (e-mail: s.golestan@ieee.org).

J. M. Guerrero is with the Department of Energy Technology, Aalborg University, Aalborg DK-9220, Denmark (e-mail: joz@et.aau.dk).

of SRF-PLL as a filter or controller inside the closed-loop control systems despite the great advantages that it can offer.

In this paper, the transfer function describing the actual input-output relationship of the conventional SRF-PLL is presented. This transfer function shows that the conventional SRF-PLL is actually a first-order complex bandpass filter (CBF). It is worth mentioning that the complex filters have an asymmetrical frequency response around zero frequency, and therefore they can make distinction between the positive and negative sequences of a same frequency [3]-[5].

II. TRANSFER FUNCTION REPRESENTATION OF SRF-PLL

In this section, the transfer function describing the actual input-output relationship of the SRF-PLL is determined. To determine this transfer function, it is assumed that: 1) the LPF used to filter out the d-axis voltage component is a first-order LPF of the form $\text{LPF}(s) = k_v/(s + k_v)$ where k_v is the LPF cutoff frequency; and 2) the proportional gain k_p of the PI controller and the cutoff frequency k_v are equal, i.e., $k_p = k_v = k$. The second assumption is similar to that assumed in [6] to obtain the transfer function describing the input-output relationship of the Enhanced PLL (EPLL).

According to Fig. 1, the SRF-PLL output signals can be expressed in time-domain as

$$\begin{aligned}
\hat{v}_{\alpha,1}^+(t) &= \hat{v}_{d,1}^+(t) \cos\left(\hat{\theta}_1^+\right) \\
\hat{v}_{\beta,1}^+(t) &= \hat{v}_{d,1}^+(t) \sin\left(\hat{\theta}_1^+\right).
\end{aligned} \tag{1}$$

Differentiating from both sides of (1) yields

$$\begin{aligned}
\dot{\hat{v}}_{\alpha,1}^+(t) &= \dot{\hat{v}}_{d,1}^+(t) \cos\left(\hat{\theta}_1^+\right) - \dot{\hat{\theta}}_1^+ \hat{v}_{d,1}^+(t) \sin\left(\hat{\theta}_1^+\right) \\
\dot{\hat{v}}_{\beta,1}^+(t) &= \dot{\hat{v}}_{d,1}^+(t) \sin\left(\hat{\theta}_1^+\right) + \dot{\hat{\theta}}_1^+ \hat{v}_{d,1}^+(t) \cos\left(\hat{\theta}_1^+\right).
\end{aligned} \tag{2}$$

According to Fig. 1 and what was assumed at the beginning of this section, we can obtain $\dot{\hat{\theta}}_1^+$ and $\dot{\hat{v}}_{d,1}^+$ as

$$\begin{aligned}
\dot{\hat{\theta}}_1^+ &= \hat{\omega}(t) + k \frac{v_q(t)}{\hat{v}_{d,1}^+(t)} \\
\hat{v}_{d,1}^+(s) &= \frac{k}{s+k} v_d(s) \Rightarrow \dot{\hat{v}}_{d,1}^+(t) = k \left[v_d(t) - \hat{v}_{d,1}^+(t)\right].
\end{aligned} \tag{3}$$

Substituting (3) into (2) and performing some simple mathematical manipulations, yields

$$\dot{\hat{v}}_{\alpha,1}^+(t) = k \underbrace{\left\{v_d(t) \cos\left(\hat{\theta}_1^+\right) - v_q(t) \sin\left(\hat{\theta}_1^+\right)\right\}}_{v_\alpha(t)}$$

$$- k \underbrace{\hat{v}_{d,1}^+(t) \cos\left(\hat{\theta}_1^+\right)}_{\hat{v}_{\alpha,1}^+(t)} - \hat{\omega}(t) \underbrace{\hat{v}_{d,1}^+(t) \sin\left(\hat{\theta}_1^+\right)}_{\hat{v}_{\beta,1}^+(t)} \tag{4}$$
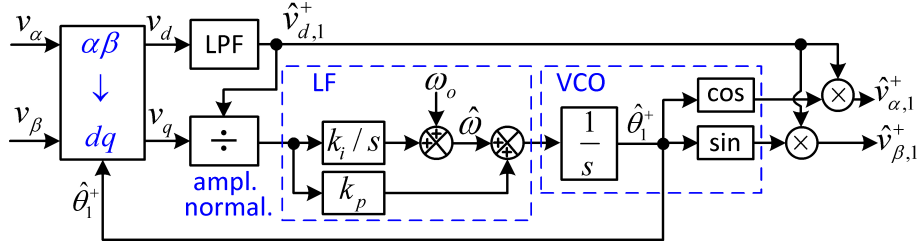
Fig. 1. Block diagram description of the conventional SRF-PLL.

$$\dot{v}_{\beta,1}^{+}(t) = k \underbrace{\left\{ v_d(t) \sin\left(\hat{\theta}_1^+\right) + v_q(t) \cos\left(\hat{\theta}_1^+\right) \right\}}_{v_\beta(t)}$$

$$- k \underbrace{\hat{v}_{d,1}^{+}(t) \sin\left(\hat{\theta}_1^+\right)}_{\hat{v}_{\beta,1}^{+}(t)} + \hat{\omega}(t) \underbrace{\hat{v}_{d,1}^{+}(t) \cos\left(\hat{\theta}_1^+\right)}_{\hat{v}_{\alpha,1}^{+}(t)}. \quad (5)$$

Using (4) and (5), the state-space description of the SRF-PLL can be obtained as

$$\begin{cases} \dot{\boldsymbol{x}}(t) = \boldsymbol{A}(t)\boldsymbol{x}(t) + \boldsymbol{B}\boldsymbol{u}(t) \\ \boldsymbol{y}(t) = \boldsymbol{C}\boldsymbol{x}(t) \end{cases} \quad (6)$$

where

$$\boldsymbol{x}(t) = \begin{bmatrix} \hat{v}_{\alpha,1}^{+}(t) \\ \hat{v}_{\beta,1}^{+}(t) \end{bmatrix}; \boldsymbol{u}(t) = \begin{bmatrix} v_\alpha(t) \\ v_\beta(t) \end{bmatrix};$$

$$\boldsymbol{A}(t) = \begin{bmatrix} -k & -\hat{\omega}(t) \\ \hat{\omega}(t) & -k \end{bmatrix}; \boldsymbol{B} = k\boldsymbol{I}; \boldsymbol{C} = \boldsymbol{I}.$$

Notice that the SRF-PLL is a time varying system, as the off-diagonal entries of the state matrix $\boldsymbol{A}$ are functions of time.

A. Analysis With Constant $\hat{\omega}$

Let us assume that the estimated frequency $\hat{\omega}$ is constant. In this case, the state matrix $\boldsymbol{A}$ is time-invariant, and therefore the state-space description of (6) can be expressed in transfer function form as

$$\boldsymbol{y}(s) = \left[\boldsymbol{C}(s\boldsymbol{I} - \boldsymbol{A})^{-1} \boldsymbol{B} \right] \boldsymbol{u}(s) \quad (7)$$

or equivalently

$$\begin{bmatrix} \hat{v}_{\alpha,1}^{+}(s) \\ \hat{v}_{\beta,1}^{+}(s) \end{bmatrix} = \frac{k}{(s+k)^2 + \hat{\omega}^2} \begin{bmatrix} s+k & -\hat{\omega} \\ \hat{\omega} & s+k \end{bmatrix} \begin{bmatrix} v_\alpha(s) \\ v_\beta(s) \end{bmatrix}. \quad (8)$$
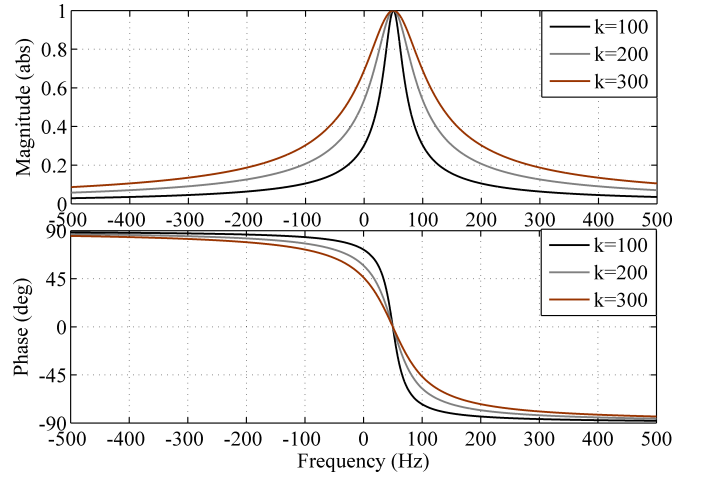
In space vector notation, (8) can be expressed as

$$\begin{aligned} \vec{v}_{\alpha\beta,1}^{+}(s) &= \frac{k\left[(s+k) + j\hat{\omega}\right]}{(s+k)^2 + \hat{\omega}^2} \vec{v}_{\alpha\beta}(s) \\ &= \frac{k[\cancel{(s+k)} + \cancel{j\hat{\omega}}]}{[\cancel{(s+k)} + \cancel{j\hat{\omega}}][(s+k) - j\hat{\omega}]} \vec{v}_{\alpha\beta}(s) \\ &= \underbrace{\frac{k}{(s - j\hat{\omega}) + k}}_{G_{\mathrm{SRF-PLL}}(s)} \vec{v}_{\alpha\beta}(s) \end{aligned} \quad (9)$$

where $\vec{v}_{\alpha\beta,1}^{+}(s) = \hat{v}_{\alpha,1}^{+}(s) + j\hat{v}_{\beta,1}^{+}(s)$ and $\vec{v}_{\alpha\beta}(s) = v_\alpha(s) + jv_\beta(s)$.

Equation (9) shows that the SRF-PLL is actually a first-order CBF. Fig. 2 shows the frequency response of (9) for

Fig. 2. Frequency response of $G_{\mathrm{SRF-PLL}}(s)$ for $\hat{\omega} = 2\pi 50$ rad/s and three-different values of k.

$\hat{\omega} = 2\pi 50$ rad/s and three-different values of k. Notice that the responses to negative frequencies in these plots can be interpreted as the responses to the negative sequence vector signal. As expected, the SRF-PLL frequency response is asymmetrical around zero frequency: it provides unity gain with zero-phase shift at the fundamental frequency of positive sequence, while it provides a certain level of attenuation at the same frequency of negative sequence.

B. Analysis With Time-Varying $\hat{\omega}$

It is shown in this section that the estimated frequency $\hat{\omega}$ is in general a slowly varying function time. Therefore, the obtained transfer function for the SRF-PLL (which was based on assuming a constant value for the estimated frequency $\hat{\omega}$) can provide a good approximation in general case. This analysis is based on the linearized model of the SRF-PLL which can be simply obtained by assuming a quasi-locked state [7].

Fig. 3 shows the linearized model of the SRF-PLL in which ω and θ_1^+ are the frequency and phase of the grid voltage, respectively. According to this model, the closed loop transfer function relating the actual frequency to the estimated frequency can be obtain as

$$\hat{\omega}(s) = \frac{k_i}{s^2 + k_p s + k_i} \omega(s). \quad (10)$$

This transfer function (which is a standard second order transfer function) implies any variation in the grid frequency
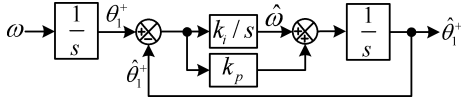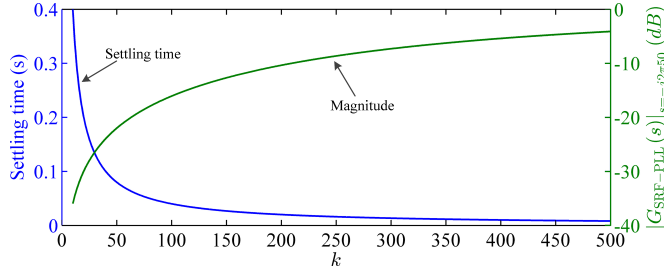
Fig. 3. Linearized model of the SRF-PLL.

Fig. 4. SRF-PLL settling-time in extraction of FFPS component as a function of k (labeling on the left); Attenuation provided by the SRF-PLL at the fundamental frequency of negative sequence as a function of k (labeling on the right).

does not appear immediately in the signal $\hat{\omega}$, and there is a transition time that is determined by the PLL's bandwidth. To ensure high noise immunity, a limited bandwidth for the PLL is typically selected. Therefore, it can be concluded that the estimated frequency $\hat{\omega}$ experiences a smooth transition when the grid frequency undergoes variations. On the other hand, in most practical cases the grid frequency ω has a stable nature, and its sudden and large variations are not expected [8]. According to this fact and that mentioned above, it can be concluded that the estimated frequency $\hat{\omega}$ is in practice a slowly varying function of time. Thus, the obtained transfer function for the SRF-PLL, which obtained by assuming a fixed $\hat{\omega}$, can provide a good approximation in general case.

III. DESIGN GUIDELINES

As shown in previous section, $G_{\text{SRF-PLL}}(s)$ is a CBF (with center frequency $\hat{\omega}$) which its bandwidth is determined by the parameter k. The higher the value of k, the higher the bandwidth and, therefore, the lower the filtering capability (see Fig. 2). So, selection of k involves a trade-off between the filtering capability and the transient time.

Assuming the dc offset in the SRF-PLL input is negligible (as is typically the case), the fundamental frequency negative sequence (FFNS) component is the disturbance component that we should be most concerned about, due to its low frequency. Fig. 4 shows the attenuation provided by the SRF-PLL at the fundamental frequency of negative sequence as a function of k. The 2% settling time of the SRF-PLL in extraction of the FFPS component (according to (9) the 2% settling time can be approximated by $t_s \approx 4/k$) is also shown in this figure. The figure clearly shows the trade-off between the filtering capability and transient time, and it can be used for selecting a proper value for k.

Once the value of k is determined, the next step is to determine the integral gain k_i. From Fig. 3, the closed-loop transfer function relating the input and estimated phases can

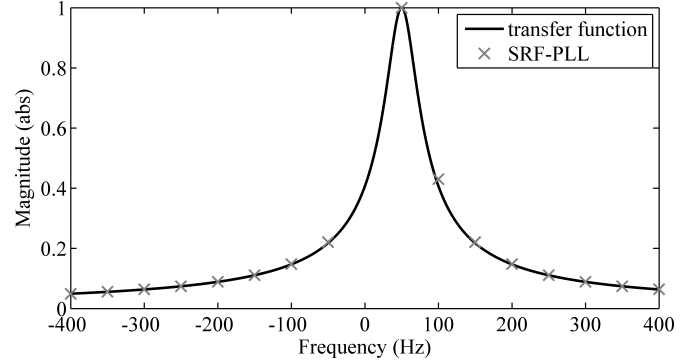| Parameter	Value
Proportional gain, k_p	140
LPF's cutoff frequency, k_v	140
Integral gain, k_i	9800
Sampling frequency, f_s	10 kHz
Nominal frequency, w_o	$2\pi 50$ rad/s

Fig. 5. Evaluation of accuracy of the obtained transfer function.

be expressed as

$$G_{cl}(s) = \frac{\hat{\theta}_1^+(s)}{\theta_1^+(s)} = \frac{k_p s + k_i}{s^2 + k_p s + k_i} \tag{11}$$

which is a standard second order transfer function, having a zero. Define $k = k_p = 2\zeta\omega_n$ and $k_i = \omega_n^2$ where ζ is the damping factor and ω_n is the natural frequency. Thus, we can write

$$k_i = \frac{k^2}{4\zeta^2}. \tag{12}$$

As the value of k has already been determined, k_i can be determined by selecting a proper value for ζ. Often $\zeta = 1/\sqrt{2}$ [7] and sometimes $\zeta = 1$ [8] is recommended in literature. The former value is selected in this paper which results in $k_i = k^2/2$.

IV. NUMERICAL RESULTS

In this section, the accuracy of obtained transfer function for the SRF-PLL is confirmed through numerical results. The selected values for control parameters are summarized in Table I.

To evaluate the accuracy of obtained transfer function, different harmonic components of different sequences are added to the input of the SRF-PLL and their amplitudes at the output of the SRF-PLL are measured. The gain of SRF-PLL at each harmonic frequency is then obtained by dividing the measured amplitude by the input voltage amplitude at that harmonic frequency, and compared with those predicted by the transfer function. Fig. 5 shows the obtained results. It can be observed that the obtained transfer function is accurate.

V. CONCLUSION

In this paper the transfer function describing the actual input-output relationship of the SRF-PLL was developed.

Using this transfer function it was shown that the conventional SRF-PLL is a first-order CBF. Usefulness of this transfer function in tuning of the SRF-PLL's control parameters was also shown.

REFERENCES

[1] S. Golestan, M. Monfared, F. D. Freijedo, and J. M. Guerrero, "Performance improvement of a prefiltered synchronous reference frame PLL by using a PID type loop filter," *IEEE Trans. Ind. Electron*. vol. 61, no. 7, pp. 3469-3479, Jul. 2014.

[2] Y. Wang and Y. Li, "Three-phase cascaded delayed signal cancellation PLL for fast selective harmonic detection," *IEEE Trans. Ind. Electron.*, vol. 60, no. 4, pp. 1452-1463, Apr. 2013.

[3] X. Guo, W. Wu, and Z. Chen, "Multiple-complex coefficient-filter-based phase-locked loop and synchronization technique for three-phase grids interfaced converters in distributed utility networks," *IEEE Trans. Ind. Electron.*, vol. 58, no. 4, pp. 1194-1204, Apr. 2011.

[4] X. Guo, W. Y. Wu, "Simple synchronisation technique for three-phase grid-connected distributed generation systems," *IET Renew. Power Gener.*, vol. 7, no. 1, pp. 55-62, Jan. 2013.

[5] X. Guo, "Frequency-adaptive voltage sequence estimation for grid synchronisation," *Electron. Lett.*, vol. 46, no. 14, pp. 980-982, Jul. 2010.

[6] M. Karimi-Ghartemani, "Linear and pseudo-linear enhanced phased-locked loop (EPLL) structures," *IEEE Trans. Ind. Electron.*, vol. 61, no. 3, pp. 1464-1474, Mar. 2014.

[7] Y. F. Wang and Y. W. Li, "Analysis and Digital Implementation of Cascaded Delayed-Signal-Cancellation PLL," *IEEE Trans. Power Electron.*, vol. 26, no. 4, pp. 1067-1080, Apr. 2011.

[8] M. Karimi Ghartemani, S. A. Khajehoddin, P. K. Jain, and A. Bakhshai, "Problems of startup and phase jumps in PLL systems," *IEEE Trans. Power Electron.*, vol. 27, no. 4, pp. 1830-1838, Apr. 2012.

Josep M. Guerrero (S'01-M'04-SM'08) received the B.S. degree in telecommunications engineering, the M.S. degree in electronics engineering, and the Ph.D. degree in power electronics from the Technical University of Catalonia, Barcelona, in 1997, 2000 and 2003, respectively. Since 2011, he has been a Full Professor with the Department of Energy Technology, Aalborg University, Denmark, where he is responsible for the Microgrid Research Program. From 2012 he is a guest Professor at the Chinese Academy of Science and the Nanjing University of Aeronautics and Astronautics; and from 2014 he is chair Professor in Shandong University.

His research interests is oriented to different microgrid aspects, including power electronics, distributed energy-storage systems, hierarchical and cooperative control, energy management systems, and optimization of microgrids and islanded minigrids. Prof. Guerrero is an Associate Editor for the IEEE TRANSACTIONS ON POWER ELECTRONICS, the IEEE TRANSACTIONS ON INDUSTRIAL ELECTRONICS, and the IEEE Industrial Electronics Magazine, and an Editor for the IEEE TRANSACTIONS on SMART GRID. He has been Guest Editor of the IEEE TRANSACTIONS ON POWER ELECTRONICS Special Issues: Power Electronics for Wind Energy Conversion and Power Electronics for Microgrids; the IEEE TRANSACTIONS ON INDUSTRIAL ELECTRONICS Special Sections: Uninterruptible Power Supplies systems, Renewable Energy Systems, Distributed Generation and Microgrids, and Industrial Applications and Implementation Issues of the Kalman Filter; and the IEEE TRANSACTIONS on SMART GRID Special Issue on Smart DC Distribution Systems. He was the chair of the Renewable Energy Systems Technical Committee of the IEEE Industrial Electronics Society. In 2014 he was awarded as ISI Highly Cited Researcher.

Saeed Golestan (M'11) received the B.Sc. degree in electrical engineering from Shahid Chamran University of Ahvaz, Iran, in 2006, and the M.Sc. degree in electrical engineering from Amirkabir University of Technology, Tehran, Iran, in 2009.

He is currently a Lecturer with the Department of Electrical Engineering, Abadan Branch, Islamic Azad University, Iran. His research interests include phase-locked loop and nonlinear filtering techniques for power engineering applications, power quality, and distributed generation systems.